

Photo-Hadronic Pair Creation In Magnetospheric Current Sheets Of Accreting Black Holes

D. Karavola¹, M. Petropoulou^{1,2}, D. F. G. Fiorillo³, L. Comisso⁴, L. Sironi⁴

¹National and Kapodistrian University of Athens, University Campus Zografos, GR 15784, Athens, Greece

²Institute of Accelerating Systems & Applications, University Campus Zografos, GR 15784, Athens, Greece

³Deutsches Elektronen-Synchrotron DESY, Platanenallee 6, 15738 Zeuthen, Germany

⁴Department of Astronomy and Columbia Astrophysics Laboratory, Columbia University, New York, NY 10027, USA

E-mail: dkaravola@phys.uoa.gr, mpetropo@phys.uoa.gr

Abstract. A ubiquitous feature of accreting black hole systems is their hard X-ray emission which is thought to be produced through Comptonization of soft photons by pairs in the vicinity of the black hole. The origin and composition of this hot plasma source, known as the corona, is a matter open for debate. In this contribution we investigate the role of relativistic protons accelerated in black-hole magnetospheric current sheets in the pair enrichment of AGN coronae. We find cases where photohadronic interactions between protons and photons in the magnetospheric region can produce enough secondary pairs to create coronae with Thomson optical depths, $\tau_T \sim 0.10 - 10$. More importantly we find a significant dependence of the secondary pair density on the Eddington ratio, defined here as the ratio of the intrinsic X-ray luminosity to the Eddington luminosity of the source. We also present the predicted high-energy neutrino spectrum and discuss our results in light of the recent IceCube observations of TeV neutrinos from NGC 1068.

1 Introduction

Active Galactic Nuclei (AGN) are the most powerful persistent sources of electromagnetic radiation in the Universe. They are powered by an accreting supermassive black hole that lies in their center. A typical radiation spectrum of an AGN (without jets) is presented in the right panel of Fig. 1, where one can identify a power-law continuum extending from keV to hundreds of keV in energy (see dashed blue line). The physical origin of the non-thermal X-ray emission has been a matter of debate for many decades [1]. The prevailing paradigm is that a population of hot electrons, which forms the so-called *corona*, Compton scatters soft (optical) photons from the accretion disk to X-ray energies (e.g. [2, 3]). Because energy losses due to inverse Compton scattering are typically fast, there should be a mechanism at place to continuously energize the electrons

Magnetic reconnection taking place in the vicinity of the black hole (see also sketch in Fig. 1) has been long proposed as a candidate process for maintaining the high temperature of electrons in the corona, also in the case of stellar mass accreting black holes (e.g. [4, 5]). Recently, [6] pointed out that if current sheets form in luminous enough accreting systems (providing high energy density of seed photons), inverse Compton cooling could keep the electron population at low temperatures ($kT_e \ll 100$ keV). Hard X-rays could still be produced by plasmoid-chain Comptonization, as this “cold” electron population is found



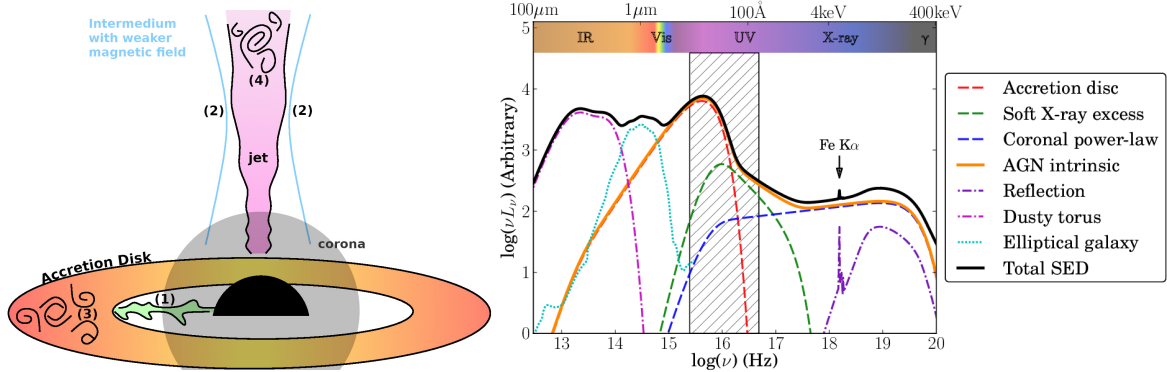


Figure 1: *Left panel:* AGN sketch showing the central massive black hole surrounded by an accretion disk. Perpendicularly to the disk a relativistic jet can be formed. A spherical corona can be shown close to the central object. The numbers in the sketch refer to: (1) magnetospheric current sheet, (2) circumnuclear medium, (3) turbulent accretion disk, and (4) jet. *Right panel:* Typical AGN electromagnetic spectrum broken down to its various components [14].

in plasmoids formed in current sheets, moving with mildly relativistic speeds. Interestingly, radiative particle-in-cell (PIC) simulations have shown that the bulk motions can mimic a quasi-thermal electron distribution with an effective temperature close to 100 keV [7, 8], while a large fraction ($\eta_X \sim 0.7$) of the dissipated magnetic energy is converted into X-ray radiation. In this context, the magnetic field strength in the coronal region can be inferred by the observed X-ray flux.

The coronal region of AGN has also been proposed as a candidate site for cosmic-ray acceleration and neutrino production (e.g., [9]). Recently, the IceCube Collaboration has presented compelling evidence for high-energy neutrino emission from NGC 1068 [10], a prototypical Seyfert galaxy at a distance of $\simeq 10.1$ Mpc, which is also a known GeV γ -ray source [11]. The neutrino emission from NGC 1068 has a soft spectrum $dN_\nu/dE_\nu \propto E_\nu^{-s}$ with $s \sim 3$, extending from $\sim 1.5 - 15$ TeV. The integrated all-flavor neutrino luminosity is $L_\nu \simeq 10^{42}$ erg/s, about 300 times lower than the estimated bolometric X-ray luminosity of the source, $L_X \sim 10^{44.5}$ erg/s [11]. An equally bright TeV γ -ray emission is not observed, suggesting that the neutrino production site should be opaque to $\gamma\gamma$ pair production. Model-independent studies conclude that hadronic processes in the coronal region of NGC 1068 are the most likely source of neutrinos [12].

Recently, [13] showed that a large-scale magnetic reconnection layer, of the order of a few gravitational radii, forming in the black-hole magnetospheric region (see sketch in Fig. 1) may be responsible for proton acceleration to tens of TeV energies. Protons interacting with coronal X-ray photons via photohadronic collisions produce TeV neutrinos, while the accompanying TeV γ rays are attenuated and cascade to lower energies, sustaining the population of electron-positron pairs that makes the corona moderately Compton thick. In this contribution we present first results from a parametric study of the neutrino emission and pair density expected from the coronal region of AGN in the presence of magnetospheric current sheets.

2 Model and Methods

In our model the X-ray emission of the corona is powered by magnetic dissipation at a large-scale magnetic reconnection layer (with typical size R of a few gravitational radii). Motivated by theory and simulations [6, 7], we express the bolometric X-ray luminosity of the corona L_X as

$$L_X = \eta_X S_{Poynt} A = \eta_X \frac{c}{4\pi} E_{rec} B A \quad (1)$$

where $\eta_X \sim 0.5$ is the fraction of the magnetic energy transferred to the X-ray photon field, S_{Poynt} is the Poynting energy flux, A is the surface of the corona boundary (taken to be $2\pi R^2$), B and $E_{rec} = \beta_{rec} B$ are respectively the magnetic field and electric field strengths in the upstream region of the layer, with $\beta_{rec} = 0.1\beta_{rec,-1}$ being the reconnection speed in units of the speed of light c . Then, the magnetic field

can be written as

$$B = \left(\frac{L_X}{\eta_X c \beta_{rec} R^2} \right)^{\frac{1}{2}}. \quad (2)$$

We assume that X-ray photons are produced via Comptonization of low-energy seed photons by pairs that are already present in the corona, but we do not attempt to model in detail the spectral formation of the X-ray coronal emission. We adopt an observationally motivated X-ray photon spectrum, namely a power law with photon index $s_X \sim 2$ extending from 0.1 keV to 100 keV,

$$n_X(\epsilon) = n_{X,0} \epsilon^{-s_X}, \quad 100 \text{ eV} \leq \epsilon \leq 100 \text{ keV}. \quad (3)$$

where $n_X(\epsilon)$ is the differential number density of photons in the corona. The X-ray spectra of AGN suggest that the optical depth for Comptonization is moderate (i.e., $\tau_T \sim 0.1-10$, [3, 15, 16]). We can therefore estimate the cold pair density that is needed to produce the assumed X-ray spectrum, $n_e = \tau_T / (\sigma_T R)$, where $\sigma_T \simeq 6.65 \cdot 10^{-25} \text{ cm}^2$ is the Thomson cross section. The magnetization of the pair plasma is then computed as

$$\sigma_e = \frac{B^2}{4\pi n_e m_e c^2} = \frac{\sigma_T L_X}{4\pi \eta_X \beta_{rec} \tau_T R m_e c^3} = \frac{\ell_X}{\eta_X \beta_{rec} \tau_T} \quad (4)$$

where ℓ_X is the X-ray compactness of the corona. Motivated by PIC simulation results of relativistic magnetic reconnection ($\sigma_e \gg 1$) we expect that any protons, if present in the upstream region of the layer, will be injected to the acceleration process, and energize at a rate $dE_p/dt = e\beta_{rec} Bc$, where $E_p = m_p \gamma_p c^2$ and γ_p is the proton Lorentz factor. The non-thermal proton number density distribution in the corona is described by a broken power law with the change of the slope happening at the proton magnetization value, $\sigma_p = B^2 / (4\pi n_p m_p c^2)$,

$$n_p(\gamma_p) = n_{p,0} \begin{cases} \sigma_p^{-s_p+1} \gamma_p^{-1}, & 1 \leq \gamma_p \leq \sigma_p \\ \gamma_p^{-s_p}, & \sigma_p < \gamma_p \leq \gamma_{\max}. \end{cases} \quad (5)$$

γ_{\max} is either determined by the confinement criterion, i.e. $\gamma_{\max} = (eB\beta_{rec}R)/(m_p c^2)$ or by the radiative cooling rate balancing the acceleration rate. The post-break power-law slope s_p is taken to be 3 or 2 (the selection and effect of these values will be discussed in section 3). We consider that a fraction η_p of the available magnetic energy density is transferred to non-thermal protons, $u_p = \eta_p u_B$. From the latter relation we can derive the normalization constant $n_{p,0}$. Finally, we can express the power injected into non-thermal protons as $L_p = u_p V c / R$, or

$$L_p = \frac{1}{3} \frac{\eta_p}{\eta_X} \frac{L_X}{\beta_{rec}} \simeq 0.67 L_X \eta_{p,-1} \eta_{X,-0.3} \beta_{rec,-1} \quad (6)$$

Parameter	Symbol (unit)	Value range
Black hole mass	$M_{bh} (M_\odot)$	$10^5 - 10^9$
Bolometric X-ray luminosity	$L_X \text{ (erg s}^{-1}\text{)}$	$10^{40} - 10^{44}$
Proton plasma magnetization	σ_p	$10^3 - 10^7$
Proton post-break slope	s_p	2 or 3
Size of reconnection layer	$R (r_g)$	3
Reconnection rate	β_{rec}	0.1
X-ray photon index	s_X	2
X-ray to magnetic energy density ratio	η_X	0.5
Non-thermal proton to magnetic energy density ratio	η_p	0.1

Table 1: Model parameters. The top three are the key parameters that we vary.

3 Results

To compute the neutrino and secondary pair density, we use the leptohadronic numerical code ATHE ν A [17]. The code solves a system of coupled integro-differential equations describing five particle species (pairs, protons, photons, neutrinos, neutrons) in a magnetized spherical corona. The range of values we use in

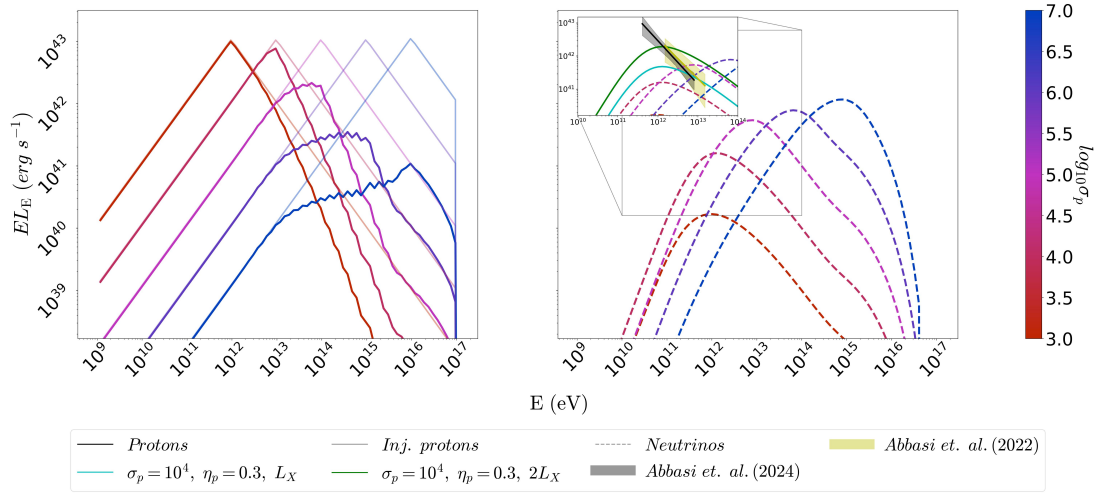


Figure 2: *Left panel:* Energy distribution for injected protons (transparent solid lines) and steady state protons (bold solid lines). *Right panel:* Energy distribution of neutrinos of all flavors (dashed lines). The color bar refers to the proton magnetization value, which determines the peak of injected proton energy distribution (see Eq. 5). The inset plot shows the best-fit power-law neutrino spectrum (with its 1σ deviation) obtained by IceCube for NGC 1068 [18, 19] and model spectra computed for different parameters. Other parameters used: $L_X = 6 \cdot 10^{42} \text{ erg s}^{-1}$ and $M_{bh} = 10^{6.7} M_\odot$.

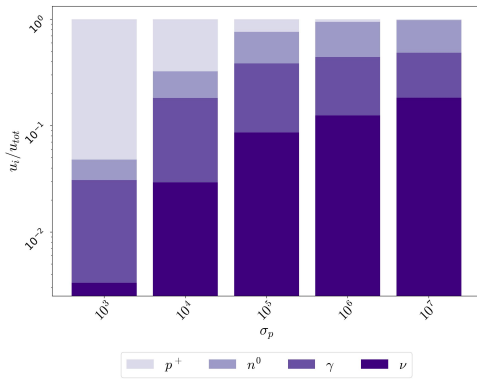


Figure 3: Stacked bar chart showing the energy density fraction of particle species i in the corona (see legend) for the same cases shown in Fig. 2. For $\sigma_p = 10^7$ the proton contribution to the total energy density is $\sim 2\%$ and therefore not visible in this representation.

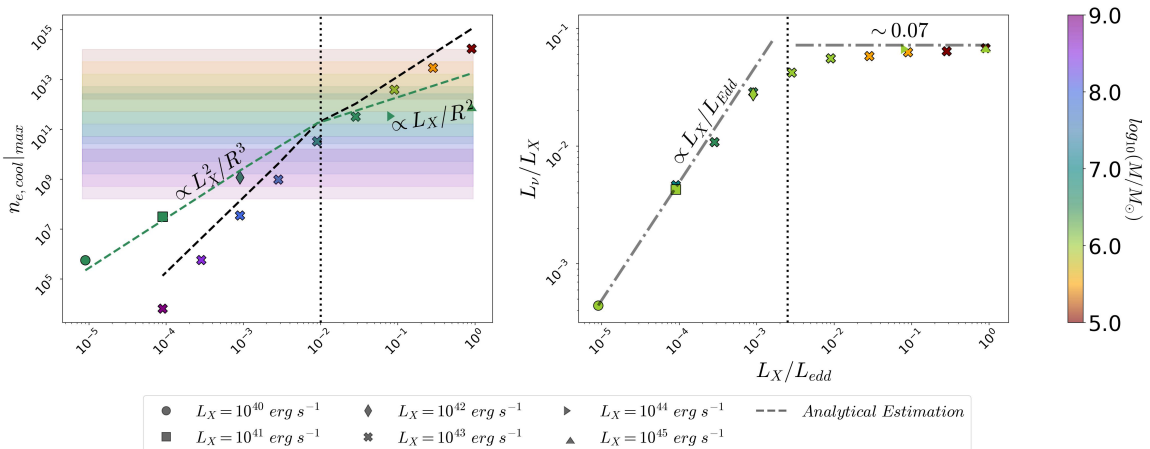


Figure 4: Total pair number density (left panel) and fraction of the neutrino luminosity over the corona X-ray luminosity (right panel) as a function of the Eddington ratio, L_X/L_{Edd} , for $\sigma_p = 10^7$.

our parametric scan are shown in Table 1. The non-thermal proton luminosity is derived from Eq. 6 ($L_p = 10^{39.5} - 10^{43} \text{ erg s}^{-1}$), and the magnetic field strength is computed using Eq. 2 ($B = 10^4 - 10^6 \text{ G}$).

In Fig. 2 we show results for varying σ_p at fixed $L_X = 6 \cdot 10^{42} \text{ erg s}^{-1}$, and $M_{bh} = 10^{6.7} M_\odot$. The energy distributions of injected protons¹ (fade solid lines) and steady state (bold solid lines) protons are shown on the left panel. We notice that as σ_p increases, the fraction of energy lost by the proton population also increases. When the the peak of the proton distribution reaches $\sim 10^{14} \text{ eV}$, photopion energy losses on coronal X-rays becomes efficient, thus softening the post-break proton spectrum. Furthermore, for high σ_p values, more energy is available for creation of secondary populations through proton-photon interactions, resulting in more luminous neutrino emission (see right panel). Meanwhile, as σ_p increases the neutrino spectrum becomes less power-law like and more log-parabolic. Fig. 3 displays, in the form of a stacked bar chart, the fraction of (bolometric) energy density carried by the proton, photon, neutron and neutrino populations at steady state for the same cases shown in Fig. 2. For $\sigma_p = 10^3$ protons that carry most of the energy of the population do not cool efficiently. As a result, they carry the largest amount of energy in the corona (dark purple). However, as σ_p increases more energy is transferred by photohadronic interactions primarily to neutrons and secondly to neutrinos, resulting from the cooling of the injected proton population, with a saturation being reached at $\sigma_p \sim 10^6$.

Fig. 4 shows the results of our parametric study. We display the total cold secondary pair number density (left) and the fraction of the bolometric neutrino luminosity (L_ν) over the bolometric X-ray corona luminosity (L_X) as a function of the Eddington² ratio L_X/L_{Edd} (right). We vary L_X while keeping a fixed black hole mass of $M = 10^7 M_\odot$ (green symbols), or we vary the black hole mass for a fixed $L_X = 10^{43} \text{ erg s}^{-1}$ (colored symbols). In all cases, we used $\sigma_p = 10^7$, $s_p=3$, and $s_X=2$. We find that for $L_X/L_{Edd} \gtrsim 10^{-2}$ the cold secondary pairs have high enough density to produce, in principle, a corona with optical depth $\tau_T \in [0.1, 10]$; this range is consistent with that inferred by the X-ray spectra of AGN (and X-ray binaries) [20, 21, 16]. Dashed lines in the left panel show our analytical prediction for the *cold (secondary)* pair number density,

$$n_{\pm}(\sigma_p, L_X, M_{bh}) \propto \begin{cases} L_X^2/M_{bh}^3, & L_X \ll L_{Edd} \\ L_X/M_{bh}^2, & L_X \gg L_{Edd} \end{cases} \quad (7)$$

which describes very well the numerical trends. The dependence on the mass comes through the coronal radius, which is taken to be a multiple of the gravitational radius. To derive the scaling relation, we assumed that photons of hadronic origin (produced indirectly via Bethe-Heitler pair production and photomeson production processes) with energies above MeV are attenuated (due to $\gamma\gamma$ pair production), leading to the creation of relativistic pairs, which cool down rapidly due to synchrotron losses, contributing to the pool of cold (secondary) pairs. In the low-Eddington ratio regime, the corona is optically thin to photohadronic interactions (non-calorimetric), hence $L_\nu \propto L_p L_X \propto L_X^2$. In the high-Eddington ratio regime we expect the protons to be calorimetric, thereby $L_\nu \propto L_p \propto L_X$. The transition is found to occur at $L_X/L_{Edd} \sim 10^{-2}$ for the chosen value of σ_p .

4 Conclusions

We outlined a model for high-energy neutrino production in AGN coronae invoking proton acceleration in a macroscopic reconnection layer in the black-hole magnetosphere. We performed a numerical parametric scan by varying three key parameters of the model, the mass of the black hole, the X-ray luminosity of the corona, and the proton plasma magnetization. We found that the Eddington ratio of the accreting system turns out to be a key parameter in determining the impact of proton-photon interactions in the corona. For systems with Eddington ratios $\gtrsim 0.01$ the corona is opaque to proton-photon interactions, leading to a significant density of cold secondary pairs. Our results have implications about the origin of pairs in coronae of AGN and stellar mass accreting systems, as well as for contribution of AGN coronae to the diffuse neutrino flux.

¹This is the distribution of protons injected by the phase of active acceleration into the neutrino production region where protons cool primarily due to photo-hadronic interactions. For more details, see [13].

²The Eddington luminosity of an accreting central object of mass M_{bh} is defined as $L_{Edd} \simeq 1.26 \cdot 10^{38} M_{bh}/M_\odot \text{ erg s}^{-1}$.

References

- [1] Matt G. X-ray Emission and Reprocessing in AGNs. In: Ho LC, Wang JW, editors. *The Central Engine of Active Galactic Nuclei*. vol. 373 of *Astronomical Society of the Pacific Conference Series*; 2007. p. 125.
- [2] Sunyaev RA, Titarchuk LG. Comptonization of X-Rays in Plasma Clouds - Typical Radiation Spectra. *A&A*. 1980 Jun;86:121.
- [3] Haardt F, Maraschi L. A Two-Phase Model for the X-Ray Emission from Seyfert Galaxies. *ApJ*. 1991 Oct;380:L51.
- [4] Beloborodov AM. Plasma Ejection from Magnetic Flares and the X-Ray Spectrum of Cygnus X-1. *ApJ*. 1999 Jan;510(2):L123-6.
- [5] Liu BF, Mineshige S, Shibata K. A Simple Model for a Magnetic Reconnection-heated Corona. *ApJ*. 2002 Jun;572(2):L173-6.
- [6] Beloborodov AM. Radiative Magnetic Reconnection Near Accreting Black Holes. *ApJ*. 2017 Dec;850(2):141.
- [7] Sironi L, Beloborodov AM. Kinetic Simulations of Radiative Magnetic Reconnection in the Coronae of Accreting Black Holes. *ApJ*. 2020 Aug;899(1):52.
- [8] Sridhar N, Sironi L, Beloborodov AM. Comptonization by reconnection plasmoids in black hole coronae I: Magnetically dominated pair plasma. *MNRAS*. 2021 Nov;507(4):5625-40.
- [9] Eichler D. High-energy neutrino astronomy: a probe of galactic nuclei? *ApJ*. 1979 Aug;232:106-12.
- [10] IceCube Collaboration, Abbasi R, Ackermann M, Adams J, Aguilar JA, Ahlers M, et al. Evidence for neutrino emission from the nearby active galaxy NGC 1068. *Science*. 2022 Nov;378(6619):538-43.
- [11] Padovani P, Resconi E, Ajello M, Bellenghi C, Bianchi S, Blasi P, et al. Supermassive black holes and very high-energy neutrinos: the case of NGC 1068. *arXiv e-prints*. 2024 May:arXiv:2405.20146.
- [12] Murase K. Hidden Hearts of Neutrino Active Galaxies. *ApJ*. 2022 Dec;941(1):L17.
- [13] Fiorillo DFG, Petropoulou M, Comisso L, Peretti E, Sironi L. TeV Neutrinos and Hard X-Rays from Relativistic Reconnection in the Corona of NGC 1068. *ApJ*. 2024 Jan;961(1):L14.
- [14] Collinson JS, Ward MJ, Landt H, Done C, Elvis M, McDowell JC. Reaching the peak of the quasar spectral energy distribution – II. Exploring the accretion disc, dusty torus and host galaxy. *MNRAS*. 2016;465:358-82.
- [15] Ricci C, Ho LC, Fabian AC, Trakhtenbrot B, Koss MJ, Ueda Y, et al. BAT AGN Spectroscopic Survey - XII. The relation between coronal properties of active galactic nuclei and the Eddington ratio. *MNRAS*. 2018 Oct;480(2):1819-30.
- [16] Petrucci PO, Gronkiewicz D, Rozanska A, Belmont R, Bianchi S, Czerny B, et al. Radiation spectra of warm and optically thick coronae in AGNs. *A&A*. 2020 Feb;634:A85.
- [17] Dimitrakoudis S, Mastichiadis A, Protheroe RJ, Reimer A. The time-dependent one-zone hadronic model - First principles. *A&A*. 2012;546:A120.
- [18] Abbasi R, Ackermann M, Adams J, Agarwalla SK, Aguilar JA, Ahlers M, et al. IceCube Search for Neutrino Emission from X-ray Bright Seyfert Galaxies. *arXiv e-prints*. 2024 Jun:arXiv:2406.07601.
- [19] Abbasi R, et al. Evidence for neutrino emission from the nearby active galaxy NGC 1068. *Science*. 2022 Nov;378(6619):538-43.
- [20] Zdziarski AA. Radiative Processes and Geometry of Spectral States of Black-Hole Binaries. *arXiv*; 2000. *ArXiv:astro-ph/0001078*.
- [21] Malzac J, Beloborodov AM, Poutanen J. X-ray spectra of accretion discs with dynamic coronae. *Monthly Notices of the Royal Astronomical Society*. 2001 Sep;326(2):417-27.